Delft University of Technology

Delft Center for Systems and Control

Technical report 25-005

Model Predictive Control of Feed Rate for Stabilizing and Enhancing Biogas Production in Anaerobic Digestion Under Meteorological Fluctuations*

A. Moradvandi, S. Heegstra, P. Ceron-Chafla, B. De Schutter, E. Abraham, and R. E. F. Lindeboom

To cite this work, please refer to the published version:
A. Moradvandi, S. Heegstra, P. Ceron-Chafla, B. De Schutter, E. Abraham, and R. E. F. Lindeboom, "Model predictive control of feed rate for stabilizing and enhancing biogas production in anaerobic digestion under meteorological fluctuations," *Journal of Process Control*, vol. 147, p. 103375, 2025. doi:10.1016/j.jprocont.2025.103375

Delft Center for Systems and Control
Delft University of Technology
Mekelweg 2, 2628 CD Delft
The Netherlands
phone: +31-15-278.24.73 (secretary)
URL: https://www.dcsc.tudelft.nl

* This report can also be downloaded via https://dspub.eu/25-005

Model predictive control of feed rate for stabilizing and enhancing biogas production in anaerobic digestion under meteorological fluctuations

Ali Moradvandi[a,b,*], Sjoerd Heegstra[a], Pamela Ceron-Chafla[a,c], Bart De Schutter[b], Edo Abraham[a], Ralph E. F. Lindeboom[a]

[a]*Department of Water Management,Delft University of Technology, Stevinweg 1, 2628 CN, Delft, The Netherlands*
[b]*Delft Center for Systems and Control, Delft University of Technology, Mekelweg 2, 2628 CD, Delft, The Netherlands*
[c]*Hoogheemraadschap van Rijnland, Archimedesweg 1, 2333 CM, Leiden, The Netherlands*

Abstract

Temperature plays a critical role in performance and stability of anaerobic digestion processes, subject to frequent meteorological fluctuations. However, state-of-the-art modeling and process control approaches for anaerobic digestion often do not consider the temporal dynamics of the temperature, which can influence microbial communities, kinetics, and chemical equilibrium, and consequently, biogas production efficiency. Therefore, to account for anaerobic digesters operating under fluctuating meteorological conditions, the Anaerobic Digestion Model no. 1 (ADM1) is mechanistically extended in this paper to incorporate temporal changes into temperature-dependent parameters by defining inhibition functions for microbial activities using the cardinal temperature model, and accounting for the lag in microbial adaptation to temperature fluctuations using a time-lag adaptation function. Thereafter, given that temperature fluctuations are a significant disturbance, a control framework based on Model Predictive Control (MPC) is developed to regulate the feeding flow rate and to ensure stable production rates despite temperature disturbances without relying on direct temperature control. An adaptive MPC approach is formulated based on a linear input-output model, where the parameters of the linear model are updated online to capture the nonlinear dynamics of the process and frequent changes in the dynamics accurately. In addition, a fuzzy logic system is employed to assign a reference trajectory for the production rate based on the temperature and its rate of change. Integrating this fuzzy logic system with the MPC controller enhances the production rate on warm days and avoids the operational failure in production on cold days. Additionally, to enhance biogas production rates, the feasibility of utilizing a portion of the produced biogas for external heating purposes is also investigated. It is demonstrated that by utilizing the proposed MPC approach, the additional amount of feed for the digester to produce methane required for a self-consumption biogas-fueled heating system can be calculated according to the meteorological variations. This enhances the process performance and stability. Finally, a thermally optimized dome digester semi-buried in the ground, operating under climate conditions of the Netherlands is considered as a case study to validate the extended model in agreement with biological and physicochemical behaviors of real-world applications, and to demonstrate the effectiveness of the proposed control system in handling temperature changes and enhancing performance.

Keywords: Anaerobic digestion, Mechanistic modeling, Model predictive control, Process control, Wastewater treatment process

1. Introduction

Biogas as a type of renewable energy is the primary product of Anaerobic Digestion (AD), an industrial biological process technology that converts wastewater through biochemical and physio-chemical conversions into methane and carbon dioxide [1]. This biological process occurs in four stages: first, the hydrolysis of organic matter; followed by acidogenesis and next by acetogenesis of intermediate products; and finally, methanogenesis for biogas production [2]. These stages are characterized by intricate intracellular and extracellular interactions among microorganisms, as well as soluble and particulate matters. The performance of AD, i.e. the amount of biogas produced, depends on various environmental, biological, and operational parameters. This performance can be negatively impacted by not only inoperative design and inexperienced operators, but also by inevitable perturbations, drawing attention and efforts towards maximizing the efficiency despite disturbances and varying operating conditions.

The operating temperature is among the most important parameters, influencing process performance and possibly causing instability in case of continuous fluctuations and sudden perturbations [3]. Temperature fluctuations might affect biological processes including microbial activity and growth, and yields and thermodynamics, as well as physicochemical processes. In general, three main temperature domains can be considered for anaerobic digester operations, namely psychrophilic 4−15 °C, mesophilic 20−40 °C, and thermophilic 45−70 °C. The impact of temperature on anaerobic digestion has been explored from various angles in the literature [4]. These range from studies on the role of temperature on microorganisms and microbial bioconversion [5], to investigations of temperature effects on process optimization and performance [6], and analyses of the effect of temperature conditions on process sustain-

*Corresponding author. Email: a.moradvandi@tudelft.nl

ability and energy efficiency [7], all of which show the importance of temperature in this context. However, in many of these investigations, the operating temperature has been assumed to be either constant or varying in a limited range.

Mathematical simulation models provide a valuable virtual benchmark for design, monitoring, and control. This is particularly relevant for assessing the effects of temperature on biogas production, which is crucial for sustainability management, optimal digester design, and effective control. For instance, the thermal management of biogas digesters has been investigated by proposing a non-calibrated heat network model in [8]. Similarly, a thermally optimal design for large-scale biogas plants through energy analysis using a heat transfer model has been studied in [9] . Two mechanistic models with explicit temperature dependency based on two different anaerobic digestion models, AM2 and BioModel, have been proposed in [10, 3]. In [10], authors showed that by using a cardinal temperature model, coupled with a simplified anaerobic digestion model, temperature fluctuations can be reflected in the overall system behaviors, more importantly biogas prediction in the presence of seasonal changes. A novel approach to incorporating short-term and long-term temperature changes in BioModel to capture the dynamic temperature dependency on process response and biogas production has also been discussed in [3]. However, to simultaneously investigate both thermal analysis and process behaviors within a comprehensive framework, a detailed model that integrates thermal and biological aspects is still required, which has not yet been proposed in the literature.

Since the temperature within the digester can be influenced by factors such as digester design as well as environmental, meteorological, and operational conditions and fluctuations, designing a control system to maintain an optimal temperature to ensure consistent biogas production and efficient energy management is required [11]. Therefore, some studies have proposed temperature-controlled digesters by implementing various control strategies, such as internal model control based PID control [12], fuzzy-PID control [13], and adaptive neural network control [14]. However, these methods aim to regulate the temperature and to manage disturbances without incorporating biological parameters. From suitability and energy efficiency points of view, it is also very important to investigate other parameters like feeding flow rate to ensure stable biogas production. Integrating biological parameters can enhance biogas production subject to temperature perturbations. Advanced control strategies, such as model predictive control (MPC), can be a suitable candidate for this aim. Furthermore, steering the feeding profile using MPC approach to control biogas production has been proposed for various objectives, e.g. demand-orientated and load-flexible biogas production [15], robust automatic process start-up [16], and maximization of methane production rate [17]. However, temperature changes have not been considered as a potential and influential parameter in these studies.

To the best knowledge of the authors, design of an MPC controller for anaerobic digestion has not yet been considered for biogas production management, subject to meteorological perturbations and uncertainties by regulating feeding flow rate. In the current paper, to address temperature fluctuations and to assess advanced control strategies, a simulation model is developed. Anaerobic Digestion Model no. 1 (ADM1) [2], a widely accepted model for anaerobic digestion pilot plants, is extended for accounting how physio-chemical and biological parameters dynamically adapt to the operating temperature by introducing temperature inhibition functions. In addition, the operating temperature is modeled based on a heat network [8] that accounts for ambient conditions and digester configurations. These two models together take several parameters and variables into account to provide a comprehensive virtual benchmark for analyzing both thermal and biological aspects of an anaerobic digester under varying meteorological conditions. This novel proposed extension is validated against research analyzing temperature fluctuations in anaerobic digestion, demonstrating reliable results. From a process control point of view, the feeding flow rate is regulated by the adaptive MPC controller to deal with the operational temperature fluctuations caused by meteorological variations, without directly controlling the temperature. The proposed MPC approach is based on a linear input-output model. The adaptive version of MPC is adopted in order to capture the highly-nonlinear dynamics of the process and to take into account the temperature fluctuations and potential model mismatches, while providing a computationally effective framework for the MPC controller. In addition to the proposed MPC controller, the enhancement of the process productivity, i.e. biogas production rate, is considered. A fuzzy logic system, acting as an expert process supervisor, is employed to assign a reference trajectory based on the temperature variations. This has been previously used to maximize the methane production rate based on volatile fatty acids [18, 17], but in this paper, it is designed according to the digester temperature and the change rate of the temperature. Additionally, a parallel preventive inhibition action is also proposed in order to enhance the process efficiency, while dealing with temperature changes. This includes a mechanism to balance inhibitory effects of increasing ammonia concentrations and lowering pH that are associated with a disbalance between acidogenic and methanogenic conversion rates. Lastly, to maximize the biogas production rate, and to increase the net biogas production, a process management option is also investigated. It concerns the integration of active temperature management in the anaerobic digester with a biogas-fueled heating system, by regulating the extra feeding flow rate required for this heating system. The objective is to avoid severe and seasonal temperature changes, while maximizing net biogas production rate. In summary, the main contributions of the present work can be listed as follows:

- ADM1 is extended temperature-wise and integrated into a heat transfer network, in order to obtain a comprehensive model to investigate the impact of different operating temperature profiles;
- An adaptive MPC framework based on a linear input-output model to control biogas production under varying meteorological conditions by regulation of the feed-

ing flow rate is developed, as opposed to the conventional direct temperature control approach;

- A fuzzy logic system is developed based on the temperature and its rate of change over two consecutive days to assign a change value to the reference trajectory of the production rate, enhancing production when temperature rises and preventing operational failures of zero production when temperature drops due to washout;
- A preventive inhibition approach to maintain pH, integrated with the MPC framework to increase input-to-product conversion (biogas and methane yield) is proposed, in which the response to temperature fluctuations is incorporated;
- A self-consumption biogas-fueled heating system is integrated with the process in order to enhance the overall process performance; the proposed MPC framework is employed to calculate the required amount of extra feeding flow rate, and it shows a positive net biogas production.

The paper is organized as follows. In the process model (Section 2) the development of the temperature-wise extended ADM1 and its integration with a heat transfer model is discussed. In the process control section (Section 3), designing an adaptive MPC controller, assigning a reference trajectory using the fuzzy logic system, the preventive inhibition mechanism, and biogas MPC management using self-consumption biogas-fueled heating system are provided. In the simulation study (Section 4), a virtual dome digester operating in the Dutch climate is simulated using the extended model and the proposed control system is then evaluated. In the last section, conclusions are drawn.

2. Process model

Biochemical and physicochemical phenomena of anaerobic digestion have been mechanistically modeled at different levels of complexity that can be used for process dynamics analysis, and control. Among those, ADM1 is the one that describes the process in a comprehensive structure through four stages, namely: hydrolysis, acidogenesis, acetogenesis, and methanogenesis [2] and it is flexible for further model development. Although the temperature is initially considered as a constant variable within the model, the structure of ADM1 allows mechanistic extension to incorporate timely temperature dynamics. Therefore, in this section, the model extension is discussed. The extended model is considered as a benchmark to simulate the anaerobic digestion under operating temperature fluctuations and to assess the performance of the proposed control system subsequently.

2.1. Anaerobic digestion model: ADM1

The state variables of ADM1 can be represented as variables for soluble matter, S_i, particulate matter, X_i, gaseous variables, $S_{\text{gas},i}$, and ion variables, S_{i-}, in which i denotes the component name. These state variables are formulated on the basis of mass balances in a set of differential equations considering biochemical and physicochemical interactions [2]. The model's stoichiometry is determined according to chemical oxygen demand (COD). Through conversions of main composite and particulate components (total composites, X_c, carbohydrates, X_{ch}, proteins, X_{pr}, and lipids, X_{li}) and soluble components (like S_{su}) to gaseous compounds (methane, $S_{\text{gas},ch4}$, carbon dioxide, $S_{\text{gas},co2}$, and hydrogen, $S_{\text{gas},h2}$), methanogenesis can be inhibited by changes of pH, hydrogen, and free ammonia. These changes mostly affect the biochemical uptake rate, which can be formulated by inhibition functions (I_j). The model is formulated for a continuous-flow stirred tank (CSTR) with a fixed volume. A summary of the model is provided in Table 1. The model consists of several parameters that can change if the temperature is not constant, which is discussed in the next section.

2.2. Temperature dependency of the parameters: Integration of dynamical temperature

The ADM1 parameters are mostly dependent on the change of the operating temperature. In this section, the temperature dependency of ADM1 and integration of temporal temperature dynamics into this model are discussed.

physicochemical processes: The liquid-gas transfers and the acid-base reactions are temperature-dependent. Henry's constants of gases, ion/acid dissociation constants, and the partial pressure of water can be corrected by van 't Hoff's equation [2]. In other words, the temperature dependence of the equilibrium constants at temperature T, can be corrected according to a base temperature T_{base} as follows:

$$\ln\frac{K_{i,T_{\text{base}}}}{K_{i,T}} = \frac{\Delta H^o}{R}\left(\frac{1}{T} - \frac{1}{T_{\text{base}}}\right) \tag{1}$$

where $K_{i,T_{\text{base}}}$ and $K_{i,T}$ denote values of the Henry's constant at T_{base} and T, respectively, and ΔH^o and R express enthalpy of volatilization and the universal gas constant. The associated correction to ADM1 parameters is given in Table 2. Besides, the partial pressures of each gas are also related to the operating temperature, which can be written based on the ideal gas law as provided in Table 2. Furthermore, as suggested in [19], the volumetric mass transfer constant, k_{La}, can also be corrected based on the 5$^{\text{th}}$ order of the base and operating temperature ratio as expressed in Table 2.

Biochemical processes: Reaction pathways, thermodynamics, and yields are affected by temperature fluctuations, which subsequently changes microbial kinetics and the microbial population dynamics. Raising the temperature can enhance reaction rates up to their optimal point, but they will be subsequently diminished beyond that optimal temperature [2]. This works like inhibitory factors. Therefore, temperature inhibition functions are defined in this study to model dynamical effects of temperature changes on some selected biochemical processes. To model the temperature inhibition functions, I_T, the cardinal temperature equation [20] is employed as follows:

$$I_T = \frac{(T - T_{\max})(T - T_{\min})^2}{(T_{\text{opt}} - T_{\min})\left[(T_{\text{opt}} - T_{\min})(T - T_{\text{opt}}) - (T_{\text{opt}} - T_{\max})(T_{\text{opt}} - T_{\min} - 2T)\right]} \tag{2}$$

Table 1: Summary of ADM1; processes are divided into biochemical, ρ_i, physio-chemical, $\rho_{AB,i}$, and liquid-gas, $\rho_{T,i}$, processes with $\nu_{i,j}$ as stoichiometric coefficients; q denotes the flow rate; k_{dis}, $k_{hyd,i}$, $k_{m,i}$, $K_{S,i}$, and $k_{dec,i}$ express disintegration, hydrolysis, maximum uptake, half saturation coefficient, and biomass decay rates, respectively; I_i denotes the inhibition function; $K_{a,i}$ and k_{AB,i^-} denote acid dissociation, and acid-base kinetic constants; q_{gas} and V_{gas} denote gaseous flow rate and volume, while V_{liq} expresses the liquid volume; and k_La is the volumetric mass transfer rate and $P_{\text{gas},i}$ and K_H denote the partial gas pressure and the Henry's constant.

Process	Variable	Variable description	Rate Expression (ρ)	Mass balance ($\frac{d}{dt}$)
Disintegration	X_c	Composites	$k_{dis}X_c$	Expression (1)[1]
-	S_I	Soluble inerts	-	Expression (2)[2]
	X_I	Particulate inerts		Expression (1)[1]
Hydrolysis	X_{ch}	Carbohydrates	$k_{hyd,i}X_i$	Expression (1)[1]
	X_{pr}	Protein		
	X_{li}	Lipid		
Acidogenesis	S_{su}	Monochaccharides (sugars)	$k_{m,i}\frac{S_i}{K_{S,i}+S_i}X_iI_i$	Expression (2)[2]
	S_{aa}	Amino acids		
	S_{fa}	Fatty acids		
Acetogenesis	S_{va}	Valerates	$k_{m,i}\frac{S_i}{K_{S,i}+S_i}X_iI_i$	Expression (2)[2]
	S_{bu}	Butyrates		
	S_{pro}	Propionates		
Methanogenesis	S_{Ac}	Acetate	$k_{m,i}\frac{S_i}{K_{S,i}+S_i}X_iI_i$	Expression (2)[2]
	S_{h2}	Soluble hydrogen		
	S_{ch4}	Soluble methane	-	
Death/Growth	X_{su}	Sugar degraders	$k_{dec,i}X_i$	Expression (1)[1]
	X_{aa}	Amino acids degraders		
	X_{fa}	Fatty acids degraders		
	X_{c4}	Valerate and butyrate degraders		
	X_{pro}	Propionate degraders		
	X_{ac}	Acetate degraders		
	X_{h2}	Hydrogen degraders		
Acid-base conversion	S_{cat}	Cations	$k_{AB,i^-}\left[S_{i^-}(K_{a,i}+S_{H^+})-K_{a,i}S_i\right]$	Expression (3)[3]
	S_{an}	Anions		
	S_{va^-}	Valerates ion		
	S_{bu^-}	Butyrates ion		
	S_{pro^-}	Propionates ion		
	S_{ac^-}	Acetate ion		
	S_{hco3^-}	Bicarbonate		
	S_{nh3}	Ammonia		
	S_{IC}	Inorganic carbon		
	S_{IN}	Inorganic nitrogen		
Liquid-gas transfer	$S_{\text{gas},h2}$	Hydrogen gas	$k_{\text{L}}a(S_i-K_HP_{\text{gas},i})$	Expression (4)[4]
	$S_{\text{gas},ch4}$	Methane gas		
	$S_{\text{gas},co2}$	Carbon dioxide gas		

[1] Expression (1): $\frac{q}{V_{\text{liq}}}X_{in,i}-\frac{X_i}{t_{rest}+V_{liq}/q}+\sum_j\rho_j\nu_{i,j}$

[2] Expression (2): $\frac{q}{V_{\text{liq}}}+(S_{in,i}-S_i)+\sum_j\rho_j\nu_{i,j}$

[3] Expression (3): $\frac{q}{V_{\text{liq}}}+(S_{in,i^-}-S_{i^-})-\rho_{AB,i}$

[4] Expression (4): $-\frac{q_{\text{gas}}}{V_{\text{gas}}}S_{\text{gas,i}}+\frac{V_{\text{liq}}}{V_{\text{gas}}}\rho_{T,i}$

in which T, $T_{\max}$, $T_{\min}$, and T_{opt} denote the operating temperature, the maximum and the minimum temperatures. Inspired by the standard density function of a *beta-distribution*, the cardinal temperature function includes three parameters to form the biological response to the temperature variable, T. $T_{\max}$ and $T_{\min}$ define the temperature limits below and above which the growth rate is assumed to be zero, respectively. Meanwhile, T_{opt} represents the optimal temperature that the maximum growth rate occurs. By identifying appropriate parameters, this function is able to describe the microbial activities; begins to increase gradually at $T_{\min}$, grows approximately linearly to reach T_{opt}, and decreases with rising the temperature and eventually ceases upon reaching $T_{\max}$, in line with biological understanding.

This inhibition function is included into ADM1 for hydrolysis kinetic rate constants and maximum uptake rates of acidogenesis, acetogenesis, and methanogenesis as given in Table 2. Although each component can have its own inhibition function, for the sake of simplicity and lack of available experimental data, 5 temperature inhibition functions, i.e. hydrolysis of carbohydrates, protein, and lipid ($I_{T,\{ch,pr,li\}}$), acidogenesis of sugars, amino acids, and fatty acids ($I_{T,\{su,aa,fa\}}$), acetogenesis of valerate and butyrate ($I_{T,c4}$), acetogenesis of propionate ($I_{T,pro}$), and methanogenesis of acetate and hydrogen ($I_{T,\{ac,h2\}}$), are calibrated based on the data set given in [21, 22]. In other words, the corresponding inhibition function for each stage of anaerobic digestion is determined by applying the nonlinear least squares method to identify parameters $T_{\max}$, $T_{\min}$, and T_{opt} of the cardinal function expressed by (2).

Temperature adaptation: The operating temperature can vary substantially day-by-day in some regions, subject to diverse variations in meteorological conditions. Although the response of physicochemical processes is fast, the microbial growth rates as biochemical processes require more time to adapt themselves to new conditions [3]. As suggested in [3], an

effective temperature (T_{eff}) according to the operating temperature and an adaptation constant (τ) can be defined as follows:

$$\frac{dT_{\text{eff}}}{dt} = \frac{T_{\text{eff}} - T}{\tau} \tag{3}$$

Therefore, the effective temperature is used for the correction of not only the methanogenesis pathways, as the most sensitive pathways to temperature perturbations [23], but also for other microbial growth rates [3]. The effective temperature is also considered for the design of the fuzzy logic system, which will come later. In other words, the effective temperature (T_{eff}) is the main digester temperature to be taken into account. The operating temperature (T) is only utilized for temperature corrections of dissociation, ionization, and gas-liquid mass transfer.

2.3. Thermal balance model: heat transfer network

The main mathematical model is ADM1 with the dynamical temperature extension as explained above. However, another model is required to simulate the operating temperature over a specific period of time. The operating temperature (T) is the substrate liquid temperature of the digester, which may be influenced by meteorological conditions and the design of the reactor. Therefore, a thermal/energy balance model should be provided to simulate it. This is carried out by a thermal balance digester model, inspired by the heat transfer network introduced in [8]. A dynamical thermal model for the expression of the state variable, denoted by T, can be written as follows:

$$\rho_{\text{liq}} C_{\text{liq}} V_{\text{liq}} \frac{dT}{dt} = Q_{\text{IRR}} + Q_{\text{ADV}} + Q_{\text{CON}} + Q_{\text{RAD}} + Q_{\text{EX}}, \tag{4}$$

where ρ_{liq} and C_{liq} denote the density of the digester substrate and specific heat capacity of the substrate, respectively. Various forms of heat transfers are summarized in Table 3.

3. Process control

In this section, we discuss a step-by-step design of an advanced control system for anaerobic digestion under temperature fluctuations. In order to do so, we first define the control problems. As mentioned in the original ADM1 development report [2], three operational strategies with respect to temperature can be considered: (i) temperature-controlled digestion with minor (±3 °C) changes, (ii) variable-temperature digestion with temperature changes in one specific range, (iii) variable-temperature digestion with temperature changes between mesophilic and thermophilic conditions. In second and third operational conditions, no temperature control is applied. Considering the conventional temperature ranges and realistic meteorological perturbations, the third operational scenario may be seen less often in real-world applications, as a digester working in two distinct temperature ranges may not be efficient as well. Therefore, the first two can be considered for designing a control system configuration. As far as the authors are aware of, most of the proposed control methods in the literature are meant to control the temperature of the digester as a temperature-controlled system, which is not really an anaerobic digestion control problem, while it is a “temperature control" or "temperature regulation” problem. Therefore, in this paper, we develop a control system for digestion considering the second operating scenario with new control objectives such as maximizing total biogas production (in this case, methane) subject to the varying operational temperature using feeding flow rate regulation. In this scenario, two cases, namely a constant set-point, and a reference trajectory are taken into account for the design of a control system. In the first case, the controller should be able to maintain biogas production at the given set-point, even if the operational temperature varies. In the second case, in addition to the objective in case one, a reference trajectory is assigned according to the operational temperature based on a fuzzy logic system. This approach enhances productivity when the temperature rises and reduces the risk of zero production (washout) when the temperature drops. Furthermore, we define an operational strategy using self-consumption biogas-fueled heating to bring the process to the first operational scenario in order to be able to increase the value of the constant set-point, and consequently improve the productivity during operation. The buildup of the control system is discussed in the next sections.

3.1. Model predictive control: main controller

The primary control objective is to control biogas production, while the operating temperature fluctuates within a specific temperature range, by regulating the feeding flow rate without temperature control. From the control point of view, the feeding flow rate is the most feasible control action in practice. The MPC strategy can be an appropriate candidate, as it anticipates process responses and takes control action accordingly to prevent operation failure [13]. MPC control is model-based. However, the developed mechanistic model is too complex and computationally expensive to be used for MPC control. As an alternative, a linear input-output model can be utilized instead [25, 17]. To properly capture the plant’s dynamics with this simpler model, its parameters should be updated at each time step based on new and past observations of the input and output variables. In addition, as the plant is subject to temperature changes, employing an adaptive prediction model can mimic these changes at every time step. Therefore, the adaptive MPC control is utilized to incorporate these aforementioned characteristics of the process. It should be noted that once the parameters are set for a particular time step, they are fixed over the prediction horizon for the calculation of the control actions.

According to the MPC framework, the control action is calculated for a control horizon (N_u) that minimizes a cost function based on a prediction horizon (N_p). The cost function, J, and the process constraint are, then, defined as follows:

$$J = \sum_{j=1}^{N_p} \delta \left[y(k+j|k) - w(k+j) \right]^2 + \sum_{j=1}^{N_u} \lambda \left[\Delta u(k+j-1) \right]^2 \tag{5a}$$

$$\text{s.t.} \quad u_{min} \leq u(k) \leq u_{max}, \tag{5b}$$

where $y(k)$ denotes the $j-$step ahead prediction of the output of

Table 2: Temperature dependency of the various ADM1 parameters and corresponding correction expressions according to the operating temperature (T) and the base temperature (T_{base}). Base temperature (T_{base}) and operating temperature (T) should be given on Kelvin.

Parameter description	Notation	Expression	Unit	Correction description	Reference
Ion constant of water	K_w	$10^{-14}\text{exp}\left(\frac{55900}{100R}\left(\frac{1}{T_{\text{base}}}-\frac{1}{T}\right)\right)$	M	van 't Hoff's equation	[2]
Acid dissociation constant of carbon dioxide	$K_{a,co2}$	$10^{-6.35}\text{exp}\left(\frac{7646}{100R}\left(\frac{1}{T_{\text{base}}}-\frac{1}{T}\right)\right)$	M	van 't Hoff's equation	[2]
Acid dissociation constant of inorganic nitrogen	$K_{a,IN}$	$10^{-9.25}\text{exp}\left(\frac{51965}{100R}\left(\frac{1}{T_{\text{base}}}-\frac{1}{T}\right)\right)$	M	van 't Hoff's equation	[2]
Henry's constant of methane	$K_{H,ch4}$	$0.035\text{exp}\left(\frac{-19410}{100R}\left(\frac{1}{T_{\text{base}}}-\frac{1}{T}\right)\right)$	M bar^{-1}	van 't Hoff's equation	[2]
Henry's constant of carbon dioxide	$K_{H,co2}$	$0.0014\text{exp}\left(\frac{-14240}{100R}\left(\frac{1}{T_{\text{base}}}-\frac{1}{T}\right)\right)$	M bar^{-1}	van 't Hoff's equation	[2]
Henry's constant of hydrogen	$K_{H,h2}$	$7.8^{-4}\text{exp}\left(\frac{-4180}{100R}\left(\frac{1}{T_{\text{base}}}-\frac{1}{T}\right)\right)$	M bar^{-1}	van 't Hoff's equation	[2]
Volumetric mass transfer coefficient	k_{L^a}	$k_{L^a} = k_{L^a,\text{base}}\left(\frac{T}{T_{\text{base}}}\right)^5$	d^{-1}		[19]
Partial gas pressure of water	$P_{\text{gas},h2O}$	$0.0313\text{exp}\left(5290\left(\frac{1}{T_{\text{base}}}-\frac{1}{T}\right)\right)$	bar	van 't Hoff's equation	[2]
Partial gas pressure of methane	$P_{\text{gas},ch4}$	$S_{\text{gas},ch4}\frac{RT}{64}$	bar	Ideal gas equation	[24]
Partial gas pressure of carbon dioxide	$P_{\text{gas},co2}$	$S_{\text{gas},co2}RT$	bar	Ideal gas equation	[24]
Partial gas pressure of hydrogen	$P_{\text{gas},h2}$	$S_{\text{gas},ch4}\frac{RT}{16}$	bar	Ideal gas equation	[24]
Hydrolysis kinetic rate constant	k_{hyd}	$k_{hyd}I_T$ [1]	d^{-1}	Temperature inhibition	[20]
Maximum uptake rate of acidogenesis, acetogenesis, and methanogenesis	k_{m}	$k_m I_T$ [1]	d^{-1}	Temperature inhibition	[20]

[1] $I_T = \frac{(T-T_{\text{max}})(T-T_{\text{min}})^2}{(T_{\text{optimum}}-T_{\text{min}})[(T_{\text{optimum}}-T_{\text{min}})(T-T_{\text{optimum}})-(T_{\text{optimum}}-T_{\text{max}})(T_{\text{optimum}}-T_{\text{min}}-2T)]}$.

Table 3: Various forms of heat transfers to integrate ADM1 parameters with a dynamical operating temperature (T) through a heat transfer network.

Heat loss/gain (notation)	Expression	Heat source	Design parameter	Note
Solar irradiation (Q_{IRR})	$Q_{\text{solar}}A\eta$	Solar transmission	Surface area (A) Digester wall material absorptivity (η)	Q_{solar} can be collected from weather institutes.
Advection (Q_{ADV})	$q\rho_{\text{inf}}C_{\text{inf}}(T_{\text{inf}}-T)$	Influent temperature (T_{inf})	Influent flow rate (q)	ρ_{inf} and C_{inf} denote influent density and heat capacity.
Convection/conduction (Q_{CON})	$AU(T_{\text{ambient}}-T)$	Conductive and convective heat transfers at digester walls exposed to the ambient (T_{amb})	Surface area (A) Digester wall material	Conductive and convective series resistances (U) [1]
Radiation (Q_{RAD})	$\frac{\sigma\left(T_{\text{sky}}^4-T^4\right)}{\frac{2}{A}+2\frac{1-\epsilon_{\text{surface}}}{A\epsilon_{\text{surface}}}+\frac{1-\epsilon_{\text{sub}}}{A\epsilon_{\text{sub}}}}$	Radiative heat transfer with sky in which $T_{\text{sky}} = 0.0552T_{\text{ambient}}^{3/2}$	Surface radiative emissivity ($\epsilon_{\text{surface}}$) Substrate radiative emissivity (ϵ_{sub}) Surface area (A)	The reactor surface functions as a radiation shield of the bulk fluid
External heating(Q_{heating})	Fixed value in Watts $\dot{m}_{\text{recirculation}}C_{\text{recirculation}}(T_{\text{heater}}-T)$	Heat exchanger	Heater capacity Heating temperature (T_{heater}) Recirculation mass flow ($\dot{m}_{\text{recirculation}}$)	In case of using external heating

[1] Series resistances (U) between the bulk and the ambient can be written as $U = \frac{1}{\sum_j R_{\text{CNV},j}+\sum_j R_{\text{CND},j}+R_{\text{CNV,forced}}}$, in which

- $R_{\text{CNV},j} = \frac{1}{h_j}$ denoted the convective resistance driven by convective heat transfer coefficient (h_j) between two fluids,
- $R_{\text{CND},j} = \frac{\Delta x_j}{k_j}$ denoted conductive resistance driven by thickness of the conducting layer (Δx_j), and the thermal conductivity (k_j),
- $R_{\text{CNV,forced}}$ denoted the forced convection driven by wind speed.

the process (methane production rate) at time k, $w(k)$ expresses the future set-point or reference trajectory (i.e. set-point or reference trajectory for methane production rate) at time k, and $\Delta u(k)$ denotes the planned control input increments (i.e. change in feeding flow rate) at time k. Moreover, δ and λ are the controller design parameters representing the error and the control weighting factors. In a simple form, it is assumed that the methane production rate at time step k ($y(k)$) is a function of the feeding flow rate ($u(k)$), which can also be affected by other potential operating conditions like operating temperature. The problem constraint is also given by (5b), where u_{min} and u_{max} express the upper and lower bounds of the actuator. To simplify the problem, as suggested above, an input-output model is considered as a basis of the MPC framework. Therefore, the prediction, $\hat{y}$, of the actual output, y, is replaced in (5a) and the model function is expressed by a single-input single-output discretized parameter linear model as follows [26]:

$$A(q^{-1})y(k) = B(q^{-1})u(k), \tag{6}$$

where $A(q^{-1})$ and $B(q^{-1})$ are rational functions of the time operator q^{-1} (i.e. $q^{-z}x_k = x_{k-z}$ for $z \in \mathbb{Z}$), and they can be written as follows:

$$A(q^{-1}) = 1 + a_1q^{-1} + ... + a_{n_a}q^{-n_a}, \tag{7a}$$

$$B(q^{-1}) = b_0 + b_1q^{-1} + ... + b_{n_b}q^{-n_b}, \tag{7b}$$

in which n_a and n_b express the order of the system with respect to the outputs and the inputs, respectively. Considering $\theta = [a_1, ..., a_{n_a}, b_0, ..., b_{n_b}]^T$ as the vector of the linear functions' coefficients, the online estimation of this parameter vector at time step k, i.e. $\hat{\theta}(k)$ can be derived using the least square method as follows:

$$\hat{\theta}(k) = \hat{\theta}(k-1) + \frac{P(k-1)\phi^T(k)}{1+\phi^T(k)P(k-1)\phi(k)}(y(k)-\hat{y}(k)), \tag{8}$$

where $\phi(k)$ is the augmented vector of past input and output observations, $P(k)$ is the covariance matrix, and $\hat{y}(k)$ is the prediction output, which can be written as follows:

$$\phi(k) = [y(k-1), ..., y(k-n_a), u(k), ..., u(k-n_b)]^T, \quad (9a)$$

$$P(k) = P(k-1) + \frac{P(k-1)\phi^T(k)\phi(k)P(k-1)}{1+\phi^T(k)P(k-1)\phi(k)}, \quad (9b)$$

$$\hat{y}(k) = \phi^T(k)\hat{\theta}(k-1). \quad (9c)$$

Using this approach as discussed in [17, 26, 27], since the model is updated at every time step based on new and past observations, this adaptive scheme is an effective approach to deal with disturbances and impreciseness of simplified linear model by updating $\hat{\theta}$ and predicting $\hat{y}$ accordingly.

3.2. Assigning a reference trajectory based on a fuzzy logic system

As discussed, the primary control objective is to maintain the methane production stable even when the operating temperature varies. Therefore, an appropriate set-point (w in (5a)) determined, ensuring it is feasible to reach under all possible temperatures. Meteorological conditions may vary drastically, not only seasonally, but also diurnally, affecting the process operation. Although the proposed MPC controller aims to stabilize process production, the set-point can also be adjusted according to the operating temperature at each time step. A decision for the set-point adjustment can be made by an expert, who is aware of the process and its conditions. To design an automatic control system, a fuzzy logic system is employed to obtain an appropriate reference trajectory. The fuzzy logic system works based on IF-THEN rules that are written according to expert knowledge [28], reflecting meteorological variations on the production rate. As explained, these meteorological variations yield on varying operating and effective temperatures, thereby affecting the process performance and the production rate. In other words, if the temperature rises, the production rate can be increased, and if the temperature decreases, the production rate should be decreased, thereby adjusting the reference trajectory for the controller in order to be matched to the temperature. Since the effective temperature accounts for the temperature adaptation for biological processes, it is selected as a reference to design a fuzzy logic system.

Therefore, the effective temperature ($T_{\text{eff}}(k)$) is one input to the fuzzy logic system. The direction of effective temperature changes based on two consecutive days ($\Delta T_{\text{eff}}(k) = T_{\text{eff}}(k) - T_{\text{eff}}(k-1)$) is also considered as another fuzzy logic system input. The output of the fuzzy logic system is the value of change in trajectory ($\Delta w(k)$). The first input assigns the range of the change in the reference trajectory, and the second input determines the rate of the change. Each fuzzy logic system consists of four compartments: (i) fuzzification, (ii) inference, (iii) rule base, and (iv) defuzzification. Membership functions for the inputs are trapezoidal for the sides and Gaussian for the middle, while the membership functions for the output are all Gaussian [29]. Three, five, and seven membership functions are considered for T_{eff}, ΔT_{eff}, and Δw, respectively. A decision-making rule table that relates inputs to the output is given in Table 4. All ranges for the inputs and the output are shaped symmetrically to facilitate easy tuning of the fuzzy logic system. A Mamdani inference system and the center of gravity method are employed to convert linguistic values into a crisp numerical value during defuzzification [13]. The details of the membership functions will be given and discussed for an example in Section (4.3).

Table 4: Decision-making fuzzy rules for assigning a value for the set-point change (Δw) based on the effective temperature (T_{eff}) and the rate of the change of the effective temperature (ΔT_{eff}).

$\Delta T_{\text{eff}} \rightarrow$ $T_{\text{eff}} \downarrow$	Big negative	Negative	Zero	Positive	Big positive
Low	Big negative	Medium negative	Zero	Positive	Positive
Medium	Medium negative	Negative	Zero	Positive	Medium positive
High	Negative	Negative	Zero	Medium positive	Big positive

3.3. Parallel preventive inhibition mechanism

Biogas production and process efficiency can be significantly reduced when temperature is varying [4]. These variations trigger inhibitory factors [30], that result in a different inhibitory response by various trophic groups and lead to process acidification due to VFA accumulation [31]. For example, a specific reduction of acidogenic bacteria due to high concentration of free ammonia was observed in [32]. To deal with these situations, a few preventive inhibition actions can be taken in order to prevent the operation failure and enhance the performance of the main MPC controller. In other words, in case of either ammonia or pH-induced inhibition, this action can act as a preventive strategy. Since the feeding flow rate is utilized for biogas production within the framework of MPC, a different strategy should be considered. These strategies should be fast in response and preferably should not involve the biological processes to avoid affecting the performance of the main MPC control system. In this regard, pH adjustment by regulation of alkalinity (cations, anions and the charge balance) as a parallel physical fast process [30, 31] is a well-known strategy for preventing acidification. Furthermore, this can also be considered in association with physicochemical approaches like chemical additions [30]. Consequently, a more stable pH during operation prevents inhibition, allowing the main MPC system to regulate biogas production more effectively. Therefore, the efficiency of maintaining a constant pH with the main MPC controller will be studied in the results and discussion section, using the developed temperature-extended ADM1 model.

3.4. Biogas MPC management using self-consumption biogas-fueled heating

As biogas is a type of organic fuel that can be used for heating, burning a portion of the produced biogas from anaerobic digestion, more specifically methane, to heat up the anaerobic digester, may not only upgrade the overall process efficiency, but also prevent the aforementioned inhibitions by raising the operating temperature [6]. In other words, a biogas-fueled boiler heats up the digester to bring the process to the first operational strategy, i.e. temperature-controlled digestion with minor temperature ($\pm 3^\circ$) changes. Therefore, the digester should be fed with extra feed to produce the required methane for

the self-consumption biogas-fueled heating system. It should be noted, that temperature can fluctuate freely within the proposed boundary conditions. Since it is assumed that the fuel of the boiler is provided from produced methane, the amount of methane required for burning, i.e. $\dot{m}_{\text{burned ch4}}$, can be written as follows:

$$\dot{m}_{\text{burned ch4}} = \frac{Q_{\text{EX}}}{\eta_{\text{ch4}}\tau}, \tag{10}$$

in which η_{ch4} denotes the fuel burning efficiency or lower heating value and τ expresses the adaptation constant used in (3). Moreover, Q_{EX} represents the external heating used in (4), which can be written as follows:

$$Q_{\text{EX}} = \rho_{\text{sub}} C_{\text{sub}} V_{\text{sub}} (T_{\text{heater}} - T). \tag{11}$$

Therefore, using the MPC control system presented in Section 3.1, feeding flow rate profiles subject to temperature variations as well as different T_{heater} settings can be investigated to manage biogas production effectively, which will be discussed for a dome digester in the next section.

4. Results and discussions: A simulation study

In this section, a case study is defined to assess the temperature-wise extension of ADM1. Historical meteorological changes and perturbations are used as a benchmark to verify the response of the anaerobic digester. The proposed control strategies, including MPC controller with a constant set-point as well as a fuzzy-driven reference trajectory, and the integration of stable pH with the MPC controller are assessed on the defined case study as well. Finally, a discussion on results of biogas MPC management using biogas-fueled heating strategy is also drawn. The simulation has been conducted using MATLAB. The extended ADM1 model has been implemented as a system of ordinary differential equations, while the proposed adaptive MPC controller has been applied using its analytical solution [27], combined with the updating laws of the internal model. Additionally, the MATLAB Fuzzy Logic Toolbox has been utilized for implementing the fuzzy logic system.

4.1. A dome digester with the meteorological conditions corresponding to the Netherlands climate conditions

To verify the extended model and the proposed control strategies, a full-scale concrete dome anaerobic digester is virtually located in De Bilt, the Netherlands. The dome digester is constructed according to the full-scale thermally optimal design specifications as discussed in [9] and presented in Table 5. As [33] and [9] discussed, it concerns a semi-buried dome digester with approximately one-fourth of its surface (mostly dome part) exposed to solar radiation (Figure 1). It should be noted that this type of digesters usually do not have a direct control system. Moreover, as they are not currently in use in the Netherlands, this investigation provides its feasibility for future consideration.

Regarding meteorological and ambient conditions, three influential variables, i.e. daily mean ambient temperature (T_{ambient}), daily mean wind speed, and daily mean solar irradiation (Q_{solar}), have been taken into account due to their significant impacts. The datasets for these variables are obtained based on historical data for a 30-year period (1992-2021) from the Royal Netherlands Meteorological Institute [34]. A comprehensive heat network discussed in Section (2.3) and schematically presented in Figure 1 along with the aforementioned meteorological variables, is considered for the thermal balance and to determine daily changes in the operating temperature. As can be seen, four resistance series, i.e. air–cover–dome–biogas–substrate, soil–wall–biogas–substrate, soil–wall–substrate, and soil–floor–substrate, are defined. The conductive and convective resistances, and all parameters required to simulate the heat network, are provided in Table 6. There is also no external heating.

Table 5: Design parameters and characteristics of a semi-buried dome digester used for simulation based on optimal thermally design discussions in [9].

Parameter description	Expression	Value/Expression	Unit
Operating conditions			
Feeding flow rate (on average)	q	290	$m^3\ day^{-1}$
Influent temperature (on average)	T_{inf}	297.15	K
Soil temperature (on average at a depth of 1 m)	T_{soil}	283.15	K
Sky temperature	T_{sky}	$0.0552T_{\text{ambient}}^{3/2}$	K
Digester geometry			
Total volume	V	3761.87	m^3
Liquid/gas volume ratio	-	3.36	-
Dome surface	A_{dome}	536.81	m^2
Wall surface	A_{wall}	471	m^2
Floor surface	A_{floor}	490.62	m^2
Characteristic length (for forced convection)	L_c	13.13	m
Wall thickness	ΔX_{wall}	0.3	m
Insulation thickness	$\Delta X_{\text{insulation}}$	0.02	m

Table 6: Thermal parameters used for simulation.

Parameter description	Notation	Value/Expression	Unit	Reference
Thermal conductivity				
Wall (plain concrete walls surrounded by moist earth)	k_{wall}	1.5	$W\ m^{-1}\ K^{-1}$	[35]
Dome (plain concrete with air space plus brick facing)	k_{dome}	1.2	$W\ m^{-1}\ K^{-1}$	[35]
Insulation (fiberglass)	k_{ins}	0.04	$W\ m^{-1}\ K^{-1}$	[35]
Air	k_{ins}	0.026	$W\ m^{-1}\ K^{-1}$	[35]
Convection				
Dry wall–biogas coefficient	$h_{\text{dw-b}}$	2.15	$W\ m^{-1}\ K^{-1}$	[8]
Wet wall–biogas coefficient	$h_{\text{ww-b}}$	2.70	$W\ m^{-1}\ K^{-1}$	[8]
Biogas–substrate coefficient	$h_{\text{b-s}}$	2.20	$W\ m^{-1}\ K^{-1}$	[8]
Wet wall–substrate coefficient	$h_{\text{ww-s}}$	177.25	$W\ m^{-1}\ K^{-1}$	[8]
Floor–substrate coefficient	$h_{\text{f-s}}$	244.15	$W\ m^{-1}\ K^{-1}$	[8]
Forced (Air) convection				
Thermal conductivity	k_{air}	0.026	$W\ m^{-1}\ K^{-1}$	[36]
Dynamic viscosity	ν_{air}	1.82×10^{-5}	Pa s	[36]
Density	ρ_{air}	1.205	$Kg\ m^{-3}$	[36]
Reynolds number	Re	$\frac{\rho_{\text{air}} v_{\text{wind}} L_c}{\nu_{\text{air}}}$	–	[36]
Nusselt number	Nu	$0.037Re^{4/5}Pr^{1/3}$	–	[36]
Air–insulation convection coefficient	h_{air}	$\frac{Nu\, k_{\text{air}}}{L_c}$	$W\ m^{-1}\ K^{-1}$	[36]
Substrate/influent thermal coefficients				
Heat capacity	C_{inf}	4.179×10^3	$J\ Kg^{-3}\ K^{-1}$	[8]
Density	ρ_{inf}	1×10^3	$Kg\ m^{-3}$	[8]
Radiative parameters				
Stefan-Boltzmann constant	σ	5.67×10^{-8}	$W\ m^{-2}\ K^{-4}$	[37]
Wall emissivity	ϵ_{wall}	0.75	–	[36]
Substrate emissivity	ϵ_{sub}	0.67	–	[8]

According to the given conditions and specifications of the dome digester, the defined heat network model is simulated, and the operating and effective temperature variations over a year are depicted in Figure 2. As previously mentioned, the operating temperature will be used to adjust the temperature for the physicochemical parameters, while the effective temperature will be utilized to correct the biological parameters and to assign a reference trajectory based on the fuzzy logic system.

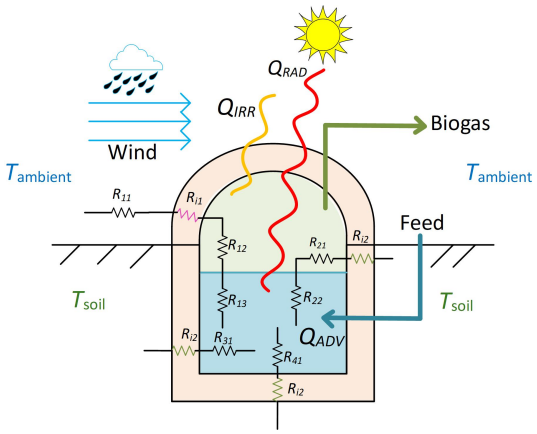

Figure 1: Schematization of the heat map of a dome digester: besides heat transfers by radiation Q_{RAD}, solar irradiation Q_{IRR}, and advection Q_{ADV} through the influent feeding to the digester, three resistance series are considered: R_{11}, R_{12}, $R_{13\text{ and }22}$, R_{21}, R_{31}, and R_{41} are the convection resistors of air–cover, dry wall–biogas, biogas–substrate, wet wall–biogas, wet wall–substrate and floor–substrate, respectively. Furthermore, R_{i1} and R_{i2} express the conduction resistors for dry and wet walls.

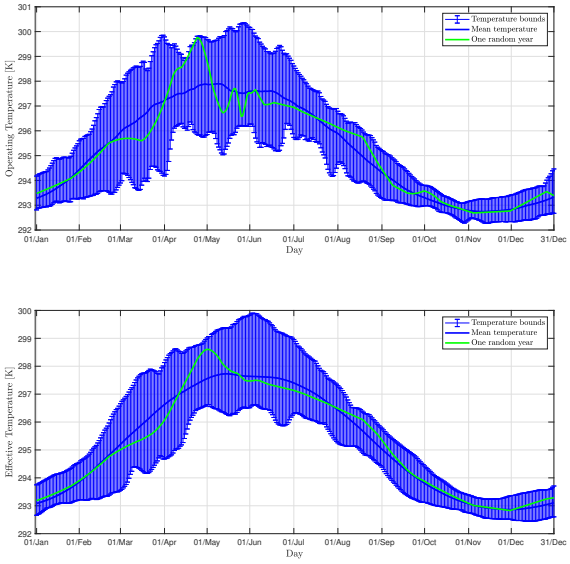

Figure 2: Operating temperature (T) and effective temperature (T_{eff}) based on 30 years historical meteorological data.

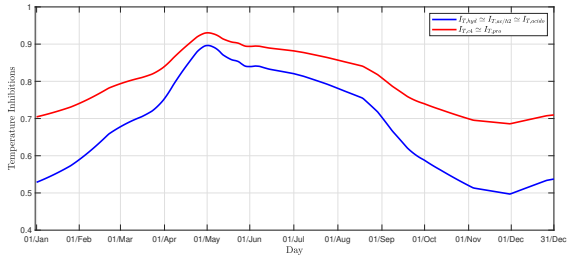

Figure 3: Variations of the temperature inhibition functions over a year.

4.2. *Simulation of a dome digester system: assessment of the proposed extended ADM1 model*

In this section, the temperature-wise extended ADM1 proposed in Section 2.1 is simulated, considering the dynamical operating and effective temperatures, reactor configurations, and other aforementioned operational conditions of the defined case study. The initial conditions are set to the default initial conditions of the original ADM1 [2], in which the substrate is protein-rich, thereby ammonia accumulation may be inevitable. Variations of the temperature inhibition functions are shown in Figure 3. These functions are calibrated based on experimental data given in [21, 22], and inhibit the maximum growth rates of hydrolysis, acidogenesis, acetogenesis, and methanogenesis of the corresponding compounds in case of a deviation from the optimal temperature. Therefore, as can be seen, they inhibit growth rates more on cold days and less when the temperature is close to the optimal level. Consequently, this is reflected in the methane production, which is depicted in Figure 4. Thus, the methane production rate is higher in a range when the temperature is relatively higher, in line with the season-based production discussed in [33]. Accumulation of fatty acids ($S_{fa} = 1.3\ \text{gL}^{-1}$ at the lowest temperature) and volatile fatty acids ($S_{va+bu+pro+ac} = 1.4\ \text{gL}^{-1}$ at the lowest temperature) occur as the temperature drops. The correlation between the fatty acid accumulation and methane production rate with temperature aligns with the findings from experimental studies conducted in [38].

While the effective temperature peaks (as shown in Figure 2 for the effective temperature), methane production does not peak (as shown in Figure 4). Based on the model output, it is anticipated that a temperature-induced increase in the hydrolysis rate constant of protein increases the free ammonia concentration and its inhibitory effect (as shown in Figure 5). This then counteracts the temperature-induced increase in methane production rate [4, 30]. Therefore, although the temperature increase suffices for more methane production, it is suppressed by free ammonia inhibition. In other words, due to the disproportionally accelerated process rates at elevated temperatures, the total concentration of free ammonia increases more than the shift in the acid-base equilibrium, and aceticlastic methanogenesis remains inhibited. It then takes some time for the methanogens to overcome the free ammonia induced inhibition, although it does not lead to significant VFA accumulation. Temperature and methane production stabilize then up till September, after which the drop in effective temperature results in significant VFA accumulation, that leads to acidification, further suppression of the growth rate and ultimately wash out (as shown in Figure 5).

4.3. *Control system assessment: discussion on MPC controller*

To assess the performance of control configuration presented in Section 3, the dome digester coupled with the proposed MPC controller is simulated in a closed loop. The objective is to maintain the methane (or biogas) production subject to meteorological fluctuations, i.e. varying operating and effective temperatures. Therefore, the performance of the proposed control strategy is evaluated based on its ability to track the assigned set-points accurately. In this regard, three yearly ran-

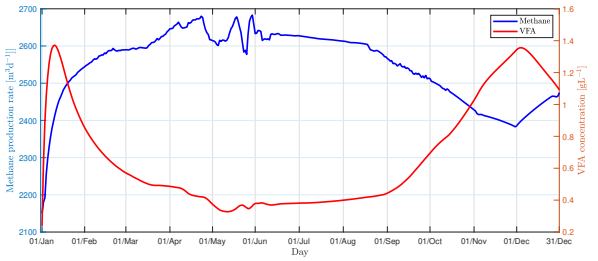

Figure 4: Variations of methane production rate and VFA concentration over a year according to the temperature fluctuations.

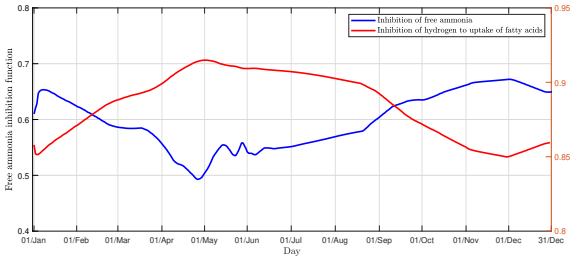

Figure 5: Variations of free ammonia inhibition function and inhibition function of hydrogen to uptake of fatty acids.

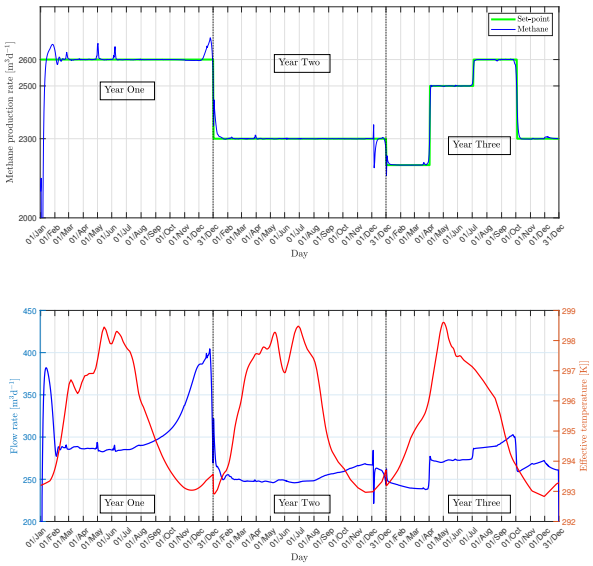

Figure 6: MPC set-point tracking subject to varying temperature | process response, and control action.

dom selected temperature scenarios from the historical data are considered, along with three different set-points for each year: constant set-points for year one (2600 $m^3\,d^{-1}$) and year two (2300 $m^3\,d^{-1}$), and step changes in the set-points for year three. The prediction and control horizons are set to 8 and 5 days, respectively. As shown in Figure 6, despite varying temperatures, the MPC controller is able to track the assigned set-points using the first order of the internal model expressed by (7a) and (7b). However, when the set-point is too high (as in year one), the controller encounters spikes at the moments of considerable changes in temperature. In contrast, with a moderate set-point (as in year two) or step-wise set-points across different seasons (as in year three), the methane production rate is smoother. As explained earlier, the motivation of the current study is to use the feeding flow rate as a biological manipulator to control methane production in response to varying temperatures, instead of controlling the temperature directly. Therefore, as shown in Figure 6, the control action varies in relation to the temperature (the higher the temperature, the lower the control action required). This outcome was expected, as temperature inhibition reduces methane production when the temperature is low. Consequently, the feeding flow rate should be increased to offset the lower growth rate by supplying more influent. However, increasing the feeding flow rate reduces the hydraulic retention time, which may increase the risk of acidification and washout [39]. On the other hand, as shown and discussed in the previous section, when the temperature is low, there is also a risk of acidification and free ammonia accumulation.

In addition to the proposed MPC controlleras discussed, the stabilized pH during operation can offset VFA and free ammonia accumulations, and consequently enhance process performance, and robustness [30]. A constant pH value can be regulated by manipulating the physicochemical processes and hydrogen ions, and adding chemical components that do not affect the biological processes. Therefore, by assuming a constant hydrogen ion concentration of 8×10^{-8} gCOD L^{-1} (i.e. pH = 7.1), the defined digester is simulated over year one to compare the results with the MPC controller that is not integrated with a constant pH. The results are shown in Figure 7. As can be seen, the inhibitory effect of free ammonia, which is a major factor preventing an increase in methane production at high temperatures, is drastically reduced. It also reduces the VFA concentration overall, particularly at low temperatures, which diminishes the risk of acidification. Consequently, the feeding flow rate required to maintain methane production (with the set-point assigned to 2600 m^3L^{-1}) is reduced by almost 20 %. This shows the advantages of a constant pH with the proposed MPC strategy.

4.4. Trajectory assignment: discussion on the fuzzy logic system

As proposed, we can use a reference trajectory assigned by the designed fuzzy logic system instead of a fixed set-point to adjust the production rate according to the effective temperature at each time step to enhance the production rate during warm days and to prevent the risk of washout during cold days. The fuzzy rules, detailed in Table 4, are designed in alignment with the biological understanding of microbial activities. In other words, an increase in effective temperature leads to an increase in microbial activity, which in turn enhances biogas production, and vice versa, following a symmetric pattern. Therefore, this can be easily transferred to other similar technologies. Since the system is tuned offline, it relies on the initial set-point for determining the trajectory. In other words, the fuzzy logic system calculates the adjustment (Δw) to be applied to the next set-point. Consequently, the initial set-point is crucial in shaping the overall trajectory. To assess the process behavior under

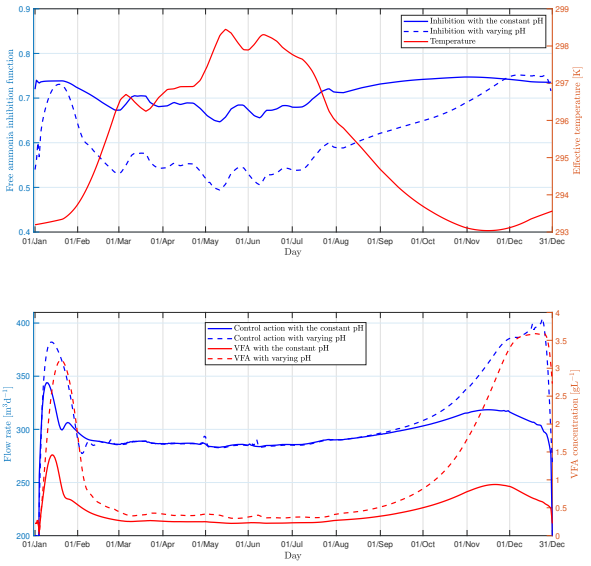

Figure 7: MPC with the constant pH and varying pH during operation | comparison of control action, VFA concentration, and free ammonia inhibition.

Table 7: Degree of membership for the fuzzy logic system.

Fuzzy set	Type	Specification
T_{eff} ([290 303])		
Low	Trapezoidal	[290 291 293 295]
Medium	Gaussian	[1.5 296.5]
High	Trapezoidal	[298 300 301 303]
ΔT_{eff} ([-0.15 0.15])		
Big negative	Trapezoidal	[-0.15 -0.12 -0.125 -0.075]
Negative	Gaussian	[0.02 -0.075]
Zero	Gaussian	[0.04 0]
Positive	Gaussian	[0.02 0.075]
Big positive	Trapezoidal	[0.075 0.125 0.13 0.15]
Δw ([-50 50])		
Big negative	Gaussian	[5 -37.5]
Medium negative	Gaussian	[5 -25]
Negative	Gaussian	[5 -12.5]
Zero	Gaussian	[5 0]
Positive	Gaussian	[5 12.5]
Medium positive	Gaussian	[5 25]
Big positive	Gaussian	[5 37.5]

different initial set-points, open-loop simulations are required. This ensures that the method is independent of skilled operators, if the initial set-point is assigned appropriately.

For this case study, the effective temperature over a 30-year period is illustrated in Figure 2. Based on the observed maximum and minimum effective temperatures, the reference temperature (T_{ref}) is defined within a range of 290 to 303 K. To accommodate values beyond these boundaries, trapezoidal membership functions are employed for the Low and High fuzzy rules. The possible range of ΔT_{ref} is determined to be between -0.15 and 0.15, with trapezoidal membership functions extending beyond these limits. Similarly, the range of Δw is set between -50 and 50 $\text{m}^3\,\text{d}^{-1}$, as larger changes between two consecutive days are considered impractical. The assigned ranges are symmetrically divided for their respective rules, ensuring balanced coverage. The specifications for the corresponding membership functions are summarized in Table 7. As depicted in Figure 8, the reference trajectory properly changes at each time step based on the effective temperature and its rate of change. As expected, at higher temperatures, the assigned production rate to be tracked is higher, and vice versa. The controller action also changes accordingly to follow the assigned reference trajectory and to offset the temperature variations. Integrating the fuzzy logic system with the adaptive MPC framework to assign the reference trajectory allows us to reduce the yearly feed by 5%, while still producing nearly the same amount of methane annually.

4.5. *Biogas management: discussion on biogas-fueled heating strategy*

As discussed above, the proposed MPC strategy can handle variations in meteorological conditions by adaptively updating the parameters of the internal linear input-output model. This approach effectively regulates the feeding flow rate to maintain a constant methane production and off-set temperature-change induced inhibition, throughout the year, despite varying operating and effective temperatures. On the other hand, using this control framework can help to estimate the amount of extra feed required to be fed to the digester to produce extra methane and use it to heat the digester. In other words, similar to the reference trajectory assigned by the fuzzy logic system discussed above, a different reference trajectory can be obtained based on the amount of external heating, as given in (10). Therefore, the control action calculated is based on this reference trajectory, provides a yearly overview of the additional influent required for feeding the digester according to temperature fluctuations. In this regard, the reference trajectory in the control framework (w) is the amount of external heating (10) at each time step. The exact amount of external heating is dependent on the design of the heating system, which specifies the heating efficiency. However, for the sake of simplification, in this case, it is assumed that the total produced amount of methane can be burned for heating to calculate only the amount of the extra feed.

According to the historical meteorological data and the corresponding simulated operating and effective temperatures depicted in Figure 2, the MPC strategy determines the amount of methane required for burning in an external heating system based on T_{heater} = 308.15 K [2, 9]. The methane requirements for the lower and upper temperature bounds, as well as for a random year are then calculated to assign a reference trajectory based on (10). Given the controller calculation, the required feeding flow rate to be fed to the digester to provide the required methane for heating is shown in Figure 9. Considering the external heating from extra methane production, the achievable effective temperature is calculated using the heat model and is also depicted in Figure 9. It shows that the daily temperature increases by 5° in average, while the temperature range (the difference between the coldest and warmest temperatures) decreases by 1.5°, which brings the digester to the temperature-controlled condition with minor (±3°) changes.

This self-consumption method can improve process perfor-

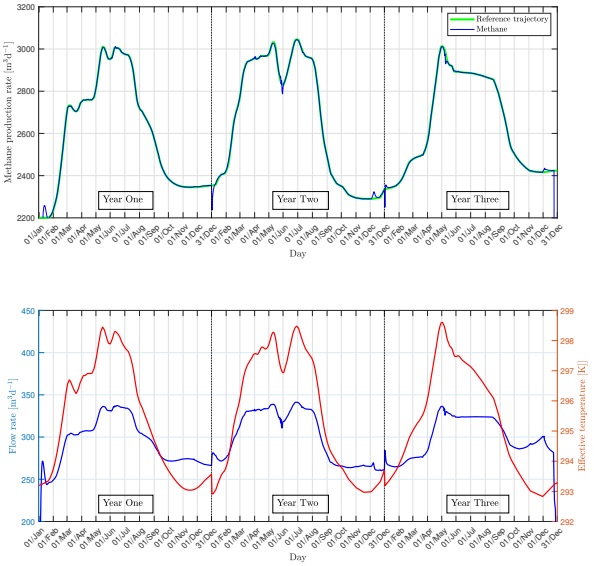

Figure 8: MPC with a reference trajectory assigned by the fuzzy logic system according to temperature variations.

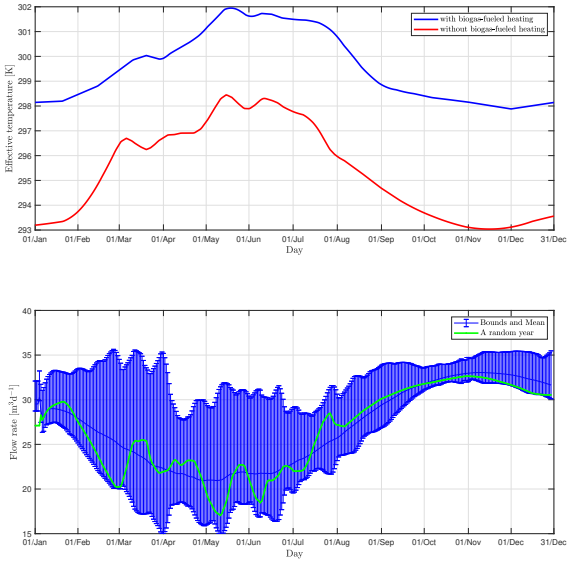

Figure 9: MPC with a reference trajectory based in the required external heating to be used as a self biogas-fueled heating system.

mance and stability in three aspects: (i) yearly feed, (ii) total COD conversion, and (iii) methane production rate. As summarized in Table 8 for the simulation of the dome digester and the developed MPC controller with and without an external heating system, using external heating reduces the total yearly required feed for the production of 2600 $m^3\,d^{-1}$, even though a portion of the produced biogas is burned for heating. This is due to an increase in COD conversion, as the effective temperature rises with external heating (Figure 9), leading to more biogas production and less VFA accumulation. On the other hand, with the increase in the effective temperature, the methane production can also be enhanced by increasing the feeding flow rate without any concern about acidification, free ammonia accumulation, and subsequent washout as can be seen in Table 8 (the potential daily methane production rate column). However, the trade-off between COD conversion and enhanced biogas production through increased feeding flow rate should also be considered [39], although it is beyond the scope of this study.

Table 8: Comparison of the digester performance with and without an external heating system for a random year; the daily potential methane production can be increased by 46%, with the almost the same amount of yearly feed.

External heating	Yearly extra feed (m^3)	Yearly feeding for daily production of 2600 $m^3\,d^{-1}$ (m^3)	Total required feed (m^3)	Potential daily methane production rate ($m^3\,d^{-1}$)
Applied	9.5616e3	1.0156e5	1.1112e5	$\lesssim$ 3800
Not applied	-	1.1159e5	1.1159e5	$\lesssim$ 2600

Thanks to the proposed MPC framework, a comparison of different heating systems in terms of heater temperature can also be investigated. As summarized in Table 9, the total required feed for a process with a heater at 308.15 K is almost 4600 m^3 higher compared to a process with a heater at 298.15 K to produce a daily methane production rate of 3000 $m^3\,d^{-1}$. However, this extra feeding enhances the process over a year in two ways: (i) improving the conversion of feed to product (with less VFA in the outputs), and (ii) increasing process stability, allowing daily production to increase to 3800 $m^3\,d^{-1}$.

4.6. Impacts and implications of the proposed methodology

Using the proposed MPC approach integrated with either a fuzzy logic system for assigning a reference trajectory or a self-sustaining biogas-fueled heating system, not only can address temperature fluctuations, but also enhance the production efficiency. It then highlights the importance and the efficiency of an integrated approach that combines MPC control of the flow rate without an external temperature control approach for AD designers and process supervisors. Such an automatic control system can also be used for processes supervised by unskilled operators. By online measurements, the control system can adapt its parameters to varying conditions and regulate the control action to stabilize and enhance the production rate. It is then proposed to apply and validate this novel temperature-wise extended model as well as the integrated automatic control framework to full-scale plants and in different geographic locations or with different digester geometries, even if they are supervised by unskilled operators as a topic for future work. It should also be pointed out that this investigation depends on meteorological conditions, which determines operating and effective temperature profiles, and therefore needs to be investigated for each specific scenario individually. In this regard, the proposed control scheme relies on expert knowledge only for the pre-analysis of historical meteorological data, initializing the fuzzy logic system, and determining an appropriate temperature for the self-heater. However, during operation, it is fully automatic, utilizing the adaptive manner to handle variations and disturbances, which ensures that the process can be effectively managed.

Table 9: Comparison of the digester performance for two different heater temperatures; increasing heater temperature increases the daily potential of methane production by 26% with less than 3% of increase in the yearly feed.

Heater temperature (K)	Yearly extra feed (m^3)	Yearly feeding for daily production of 3000 $m^3\,d^{-1}$ (m^3)	Total required feed (m^3)	Potential daily methane production rate ($m^3\,d^{-1}$)
308.15	9.5616e3	1.2018e5	1.2970e5	$\lesssim 3800$
298.15	1.9139e3	1.2385e5	1.2508e5	$\lesssim 3000$

5. Conclusions

In this paper, the anaerobic digestion model no.1 (ADM1) has been mechanistically extended in order to incorporate temporal temperature variations caused by meteorological fluctuations. The extended model demonstrates reliable outcomes in general agreement with experimental studies. On the other hand, a feeding flow rate control strategy based on MPC approach has also been proposed to deal with varying meteorological conditions and to maintain a stable methane production rate. This method can be employed in the absence of any external heating system, as it regulates the feeding flow rate to compensate for changes in the temperature. To enhance the productivity of the process under these conditions, a fuzzy logic system has been employed to assign a reference trajectory for the methane production rate for the MPC controller. This fuzzy logic system can adjust the reference trajectory to increase the production rate when the temperature rises and to reduce it when the temperature drops, thereby enhancing the process performance and avoiding operational failures. Thanks to the extended model and proposed control strategy, it has been also demonstrated that the production rate can be increased, if the pH value is fixed to deal with free ammonia and VFA accumulation. This strategy shows improvements in conversion by reducing the required feeding flow rate. Additionally, the adaptive MPC framework enables the calculation of the required extra feed to produce more methane to be used for a self-consumption biogas-fueled heating system in order to increase process performance and stability for a fixed set-point. The effectiveness of the proposed control framework has been assessed using a defined dome digester under climate conditions in the Netherlands.

Acknowledgments

The authors kindly acknowledge a research grant of the European Horizon 2020 Framework Programme (grant agreement number 821427) under the Project SARASWATI2.0.

References

[1] D. Nguyen, S. Nitayavardhana, C. Sawatdeenarunat, K.C. Surendra, and S.K. Khanal. *Biogas Production by Anaerobic Digestion: Status and Perspectives*, page 763–778. Elsevier, 2019.

[2] D.J. Batstone, J. Keller, I. Angelidaki, S.V. Kalyuzhnyi, S.G. Pavlostathis, A. Rozzi, W.T.M. Sanders, H. Siegrist, and V.A. Vavilin. The IWA anaerobic digestion model no 1 (ADM1). *Water Science and Technology*, 45(10):65–73, 2002.

[3] A. Kovalovszki, L. Treu, L. Ellegaard, G. Luo, and I. Angelidaki. Modeling temperature response in bioenergy production: Novel solution to a common challenge of anaerobic digestion. *Applied Energy*, 263:114646, 2020.

[4] Erqi Nie, Pinjing He, Hua Zhang, Liping Hao, Liming Shao, and Fan Lü. How does temperature regulate anaerobic digestion? *Renewable and Sustainable Energy Reviews*, 150:111453, 2021.

[5] R. Mei, T. Narihiro, M.K. Nobu, and W.-T. Liu. Effects of heat shocks on microbial community structure and microbial activity of a methanogenic enrichment degrading benzoate. *Letters in Applied Microbiology*, 63(5):356–362, 2016.

[6] G. Caposciutti, A. Baccioli, L. Ferrari, and U. Desideri. Biogas from anaerobic digestion: Power generation or biomethane production? *Energies*, 13(3):743, 2020.

[7] F. Calise, F.L. Cappiello, L. Cimmino, D. d'Accadia M, and M. Vicidomini. Dynamic analysis and investigation of the thermal transient effects in a cstr reactor producing biogas. *Energy*, 263:126010, 2023.

[8] S. Vilms Pedersen, J. Martí-Herrero, A.K. Singh, S.G. Sommer, and S.D. Hafner. Management and design of biogas digesters: A non-calibrated heat transfer model. *Bioresource Technology*, 296:122264, 2020.

[9] A. Ahmadi, M. Avila, and L. Barna. Pathways for the thermally optimal design and practice of anaerobic digestion in large-scale biogas plants: Heat transfer modeling and energy analysis. *Chemical Engineering Research and Design*, 197:884–907, September 2023.

[10] A. Donoso-Bravo, W.M.K.R.T.W. Bandara, H. Satoh, and G. Ruiz-Filippi. Explicit temperature-based model for anaerobic digestion: Application in domestic wastewater treatment in a uasb reactor. *Bioresource Technology*, 133:437–442, 2013.

[11] P. Garkoti, J. Ni, and S.K. Thengane. Energy management for maintaining anaerobic digestion temperature in biogas plants. *Renewable and Sustainable Energy Reviews*, 199:114430, 2024.

[12] M. Kumar, D. Prasad, B.S. Giri, and R.S. Singh. Temperature control of fermentation bioreactor for ethanol production using IMC-PID controller. *Biotechnology Reports*, 22:e00319, 2019.

[13] K. Anand, A.P. Mittal, and B. Kumar. Modelling and simulation of dual heating of substrate with centralized temperature control for anaerobic digestion process. *Journal of Cleaner Production*, 325:129235, 2021.

[14] K. Anand, A.P. Mittal, and B. Kumar. Ann-based sensorless adaptive temperature control system to improve methane yield in an anaerobic digester. *Biomass Conversion and Biorefinery*, 13(8):7265–7285, 2022.

[15] C. Dittmer, B. Ohnmacht, J. Krümpel, and A. Lemmer. Model predictive control: Demand-orientated, load-flexible, full-scale biogas production. *Microorganisms*, 10(4):804, 2022.

[16] W. Ahmed and J. Rodríguez. A model predictive optimal control system for the practical automatic start-up of anaerobic digesters. *Water Research*, 174:115599, 2020.

[17] M.A. Ghanavati, E. Vafa, and M. Shahrokhi. Control of an anaerobic bioreactor using a fuzzy supervisory controller. *Journal of Process Control*, 103:87–99, 2021.

[18] A. Robles, G. Capson-Tojo, M.V. Ruano, E. Latrille, and J.-P. Steyer. Development and pilot-scale validation of a fuzzy-logic control system for optimization of methane production in fixed-bed reactors. *Journal of Process Control*, 68:96–104, 2018.

[19] J. Lee. Development of a model to determine mass transfer coefficient and oxygen solubility in bioreactors. *Heliyon*, 3(2):e00248, 2017.

[20] L. Rosso, J.R. Lobry, and J.P. Flandrois. An unexpected correlation between cardinal temperatures of microbial growth highlighted by a new model. *Journal of Theoretical Biology*, 162(4):447–463, 1993.

[21] A. Donoso-Bravo, C. Retamal, M. Carballa, G. Ruiz-Filippi, and R. Chamy. Influence of temperature on the hydrolysis, acidogenesis and methanogenesis in mesophilic anaerobic digestion: parameter identification and modeling application. *Water Science and Technology*, 60(1):9–17, 2009.

[22] W.H. Bergland, C. Dinamarca, and R. Bakke. Temperature effects in anaerobic digestion modeling. In *Linköping Electronic Conference Proceedings*. Linköping University Electronic Press, 2015.

[23] D. Prakash, S.S. Chauhan, and J.G. Ferry. Life on the thermodynamic edge: Respiratory growth of an acetotrophic methanogen. *Science Advances*, 5(8), 2019.

[24] T. Thamsiriroj and J.D. Murphy. Modelling mono-digestion of grass silage in a 2-stage CSTR anaerobic digester using ADM1. *Bioresource Technology*, 102(2):948–959, 2011.

[25] A. Moradvandi, E. Abraham, A. Goudjil, B. De Schutter, and R.E.F. Lindeboom. An identification algorithm of switched box-jenkins systems in the presence of bounded disturbances: An approach for approximating complex biological wastewater treatment models. *Journal of Water Process Engineering*, 60:105202, 2024.

[26] G.C. Goodwin and K.S. Sin. *Adaptive filtering prediction and control*.

Courier Corporation, 2014.

[27] E.F. Camacho, C. Bordons, E.F. Camacho, and C. Bordons. *Model predictive controllers*. Springer, 2007.

[28] J.M. Mendel. Fuzzy logic systems for engineering: a tutorial. *Proceedings of the IEEE*, 83(3):345–377, 1995.

[29] L.C. De Barros, R.C. Bassanezi, and W.A. Lodwick. *First Course in Fuzzy Logic, Fuzzy Dynamical Systems, and Biomathematics*. Springer, 2016.

[30] H. Yuan and N. Zhu. Progress in inhibition mechanisms and process control of intermediates and by-products in sewage sludge anaerobic digestion. *Renewable and Sustainable Energy Reviews*, 58:429–438, 2016.

[31] D. Cysneiros, C.J. Banks, S. Heaven, and K.G. Karatzas. The effect of ph control and 'hydraulic flush' on hydrolysis and volatile fatty acids (VFA) production and profile in anaerobic leach bed reactors digesting a high solids content substrate. *Bioresource Technology*, 123:263–271, 2012.

[32] O. Yenigün and B. Demirel. Ammonia inhibition in anaerobic digestion: A review. *Process Biochemistry*, 48(5–6):901–911, 2013.

[33] R. Hreiz, N. Adouani, Y. Jannot, and M. Pons. Modeling and simulation of heat transfer phenomena in a semi-buried anaerobic digester. *Chemical Engineering Research and Design*, 119:101–116, 2017.

[34] KNMI. Knmi climate data. `http://https://www.knmi.nl/klimaat`. Accessed: 2024-06-07.

[35] L. Metcalf, H.P. Eddy, and G. Tchobanoglous. *Wastewater engineering: treatment, disposal, and reuse*, volume 4. McGraw-Hill New York, 1991.

[36] Y.A. Cengel and A. Ghajar. Heat and mass transfer (a practical approach, SI version). *McGraw-670 Hill Education*, 671(52):964, 2011.

[37] P.J. Mohr and B.N. Taylor. Codata recommended values of the fundamental physical constants: 2002. *Reviews of modern physics*, 77(1):1, 2005.

[38] D. Erdirencelebi and G.M. Ebrahimi. Enhanced sewage sludge treatment via parallel anaerobic digestion at the upper mesophilic level. *Journal of Environmental Management*, 320:115850, 2022.

[39] M.A.Khan, H.H. Ngo, W.S. Guo, Y. Liu, L.D. Nghiem, F.I. Hai, L.J. Deng, Wang J, and Y. Wu. Optimization of process parameters for production of volatile fatty acid, biohydrogen and methane from anaerobic digestion. *Bioresource Technology*, 219:738–748, 2016.